ACS APPLIED MATERIALS & INTERFACES

Research Article

www.acsami.org

Incorporation of Silver Nanoparticles into the Bulk of the Electrospun Ultrafine Polyimide Nanofibers via a Direct Ion Exchange Self-Metallization Process

Enlin Han, Dezhen Wu, Shengli Qi,* Guofeng Tian, Hongqing Niu, Gongping Shang, Xiaona Yan, and Xiaoping Yang

State Key Laboratory of Chemical Resource Engineering, Beijing University of Chemical Technology, Beijing 100029, China

Supporting Information

ABSTRACT: This paper reports our works on the preparation of the silver-nanoparticle-incorporated ultrafine polyimide (PI) ultrafine fibers via a direct ion exchange self-metallization technique using silver ammonia complex cation ($[Ag(NH_3)_2]^+$) as the silver precursor and pyromellitic dianhydride (PMDA)/4,4′-oxidianiline (4,4′-ODA) polyimide as the matrix. The polyimide precursor, poly(amic acid) (PAA), was synthesized and then electrospun into ultrafine fibers. By thermally treating the silver(I)-doped PAA ultrafine fibers, where the silver(I) ions were loaded through the ion exchange reactions of the carboxylic acid groups of the PAA macromolecules with the $[Ag(NH_3)_2]^+$ cations in an aqueous solution, ultrafine polyimide fibers embedded with silver nanoparticles with diameters less than 20 nm were successfully fabricated. The fiber-electrospinning process, the ion exchange process, and various factors influencing the hybrid ultrafine fibers preparation process such as the thermal treatment atmospheres and the thermal catalytic oxidative degradation effect of the reduced silver nanoparticles were discussed. The ultrafine fibers were characterized by attenuated total reflection-Fourier transform infrared spectroscopy (ATR-FTIR), X-ray photoelectron spectroscopy (XPS), X-ray diffraction (XRD), inductively coupled plasma atomic emission spectroscopy (ICP-AES), scanning electron microscopy (SEM), transmission electron microscopy (TEM), and thermogravimetric analysis (TGA).

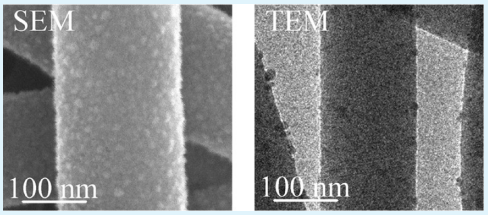

KEYWORDS: *silver nanoparticles, electrospinning, polyimide, silver ammonia*

INTRODUCTION

For preparing polymer fibers with diameters in nanometer scale, electrospinning has been demonstrated to be an efficient method.[1−3] With this technique, many kinds of polymers have been successfully electrospun into ultrafine fibers either in solution state or in melt form,[1] including nylon 6,6 (PA-6,6),[4−8] polyurethanes (PU),[9−11] polycarbonate (PC),[4,10,12−15] polyacrylonitrile (PAN),[16−19] polyvinyl alcohol (PVA),[20−22] polylactic acid (PLA),[23−26] poly(amic acid) (PAA),[27−31] polyethylene (PE),[32,33] polypropylene (PP),[34,35] and etc. While the diameters of the polymer fibers are reduced from micrometers (e.g., 10−100 μm) to submicrometers or nanometers, many amazing characteristics are emerging such as the extremely enlarged specific surface areas (over 10^3 times larger than the microfibers), flexibility in surface functionalities, high porosity, and superior mechanical performances, making the polymer nanofibers optimal candidates for many important applications. Among all the studies, the incorporation of noble nanoparticles into the ultrafine polymer fibers has attracted a great deal of attention in recent years,[7,28−31,36] since it has been anticipated and partially verified that the resulting hybrid nanofibers could be potentially applied in the fields of catalyst, drug and wound dressings, optical information storage, surface enhanced Raman scattering, and etc.[1−3,27,37]

Polyimides (PI) constitute an important class of high-performance engineering materials with excellent mechanical strength, good thermal stability, high chemical resistance, and good patterning capability.[35,36] The ultrafine PI nanofibers possess high specific surface area which lead to high filtration efficiency and can be used as the filter materials. While the silver nanoparticles have high surface activity that can form irreversible genetic material with the genetic material in bacterial cells and are used for antibacterial field.[38−40] By combining the ultrafine PI nanofibers with silver nanoparticles, the prepared PI−Ag nanofibers are reported to be promising materials in catalysis, antibacteria, and sensors.[3,28,37] A variety of methods have been developed for the incorporation of silver nanoparticles into a polymer matrix.[28−31,36,41−50] However, they can be generally divided into three classes. One is to disperse the preformed silver nanoparticles into a polymer matrix, being simple but difficult to obtain well-dispersed nanoparticles due to the easy aggregation of nanoparticles. The other is the in situ formation of silver nanoparticles through chemical or thermal reduction of the silver precursors predoped in the polymer matrix; however, the nanoparticles fabricated by

Received: February 12, 2012
Accepted: April 20, 2012
Published: April 20, 2012

Scheme 1. Ideal Synthetic Protocol for Preparing Ultrafine PMDA/ODA PI Fibers Doped with Silver Nanoparticles Using Silver Ammonia Complex Cation as the Precursor via the Direct Ion Exchange Self-Metallization Process

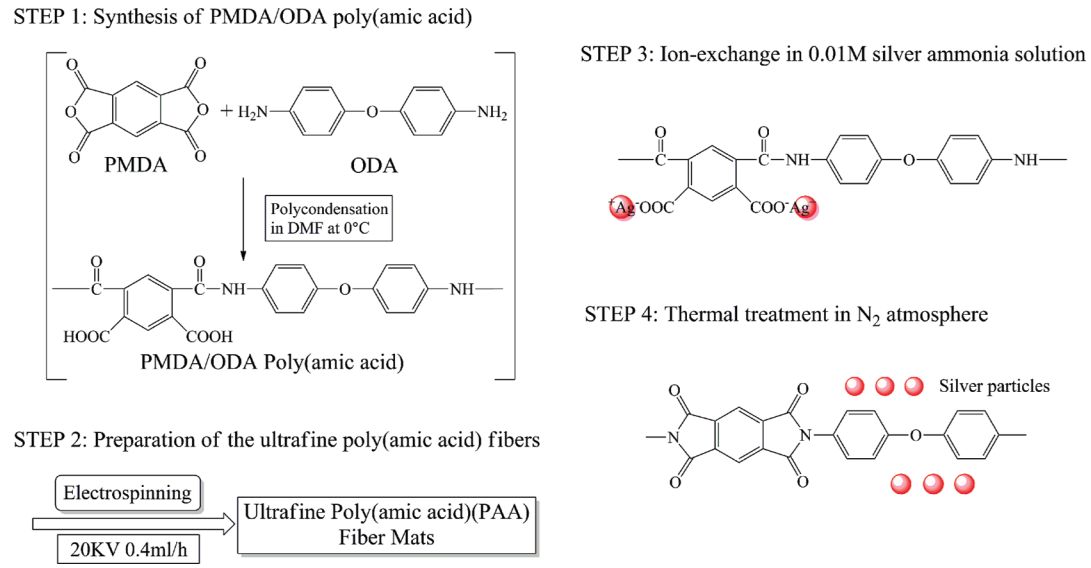

the in situ method are not surface localized but distributed in the polymer matrix. The third is the surface modification ion exchange process which is not a high efficient method.

In the present work, by employing a direct ion exchange self-metallization technique developed in our previous research,[49] which works by the use of the polyimide precursor, i.e., the electrospun poly(amic acid) (PAA) ultrafine fibers, as the starting matrix, and then by loading silver(I) into the polymer matrix through the ion exchange reactions of the carboxylic acid groups in PAA macromolecules with the silver ammonia complex cations ($[Ag(NH_3)_2]^+$), followed by thermal treatment under nitrogen environment, silver-nanoparticle-incorporated PI ultrafine fibers with good uniformity were successfully fabricated. Aqueous $[Ag(NH_3)_2]^+$ solution with a concentration of 0.01 M was selected as the silver ion sources, and the ion exchange time was confined to less than 20 s to prevent the hydrolysis and damaging effect of the alkaline $[Ag(NH_3)_2]^+$ solutions on the polymer matrix. The hybrid nanofibers were characterized by attenuated total reflection-Fourier transform infrared spectroscopy (ATR-FTIR), X-ray photoelectron spectroscopy (XPS), X-ray diffraction (XRD), inductively coupled plasma atomic emission spectroscopy (ICP-AES), scanning electron microscopy (SEM), transmission electron microscopy (TEM), and thermogravimetric analysis (TGA). The silver nanoparticles embedded in the finally prepared PI ultrafine fibers are less than 20 nm in diameters and are distributed with quite good uniformity.

EXPERIMENTAL SECTION

Reagents. Pyromellitic dianhydride (PMDA, 99%) was purchased from Shanghai Research Institute of Synthetic Resins and sublimated prior to use. 4,4′-Oxydianiline (4,4′-ODA, 99%) was purchased from Shanghai Research Institute of Synthetic Resins and recrystallized in ethyl acetate before use. *N*,*N*-Dimethylformamide (DMF, analytic pure, ≥99.5%) was purchased from Sinopharm Chemical Reagent Co. Ltd. and used as received. Ammonia solution (analytically pure, 25−28 wt %) was purchased from Sinopharm Chemical Reagent Co. Ltd. Silver nitrate ($AgNO_3$) (analytically pure, 99.8% content) was produced by Beijing Chemical Works and used as received. Silver ammonia complex cation ($[Ag(NH_3)_2]^+$) solutions were prepared in our lab by adding the dilute ammonia solution dropwise to the aqueous $AgNO_3$ solution until a transparent solution was obtained. In the present work, a 0.01 M aqueous $[Ag(NH_3)_2]^+$ solution with pH values of 9.9−10.2 was used.

Synthesis of the PMDA/ODA Poly(amic acid) Solutions. The PMDA/4,4′-ODA PAA solution was prepared by first dissolving the ODA diamine in DMF followed by the gradual addition of dianhydride with a 1 mol % excess. After intense mechanical stirring at 0 °C for 12 h, a light yellow viscous solution with 20 wt % solids was obtained. The ideal process for the polycondensation reactions was shown in Scheme 1. The inherent viscosity of the synthesized PAA resin was determined to be ca. 2.75 dL g^{-1} at 35 °C. For preparing ultrafine fibers with desirable morphologies, the synthesized PAA solution (20 wt %) was then diluted to 6, 8, 10, and 12 wt % in DMF and used for electrospinning.

Preparation of the Ultrafine Poly(amic acid) Fibers by Electrostatic Spinning. The PAA resins were then electrospun into ultrafine fibers on an electrostatic spinning apparatus. The apparatus consisted of a syringe, a spinneret which was the 12 gauge and flat-tip needle (Ø 1.1 mm hole), and a rotatable aluminum drum (Ø 100 mm) programmed with a rotating speed of 18.0 m s^{-1}. Conductive graphite paper was closely fixed onto the rotating drum and served as the substrate for collecting the ultrafine PAA fibers. A 20 kV high electric voltage was applied between the spinneret and the rotating drum using a direct-current power supplier (DWP303-1AC, China). The flow rate of the PAA resin solution was set as 0.4 mL h^{-1}, as controlled by a syringe pump (TOP5300, Japan). The distance between the spinneret and the rotating drum was 20 cm. After collection under ambient environment with constant temperature and humidity for 3 h, the ultrafine fibers were finally obtained in the form of nonwoven fabric membranes.

Fabrication of Silver-Incorporated Polyimide Nanofibers. The as-spun ultrafine PAA fiber membranes were placed in a laminar flow cabinet for 2 days to evaporate most of the remaining solvent. Then, silver ions were loaded into the ultrafine PAA fibers through ion exchange by immersing the ultrafine fiber membranes in the aqueous $[Ag(NH_3)_2]^+$ solution (0.01 M). After being rinsed thoroughly with deionized water, the silver(I)-doped membranes were thermally treated under nitrogen (N_2) atmosphere. The thermal cycles employed in the present work are heating over 2 h to 300 °C and holding constant for 2 h. Thermal treatment cycloimidizes the PAA into its final PI form and simultaneously induces silver reduction and the subsequent aggregation, forming silver nanoparticles in the nanofibers, as depicted in Scheme 1.

Characterization. The intrinsic viscosity ($[\eta]$) measurement was carried out with the use of a Germany SCHOTT 52510 Ubbelohde

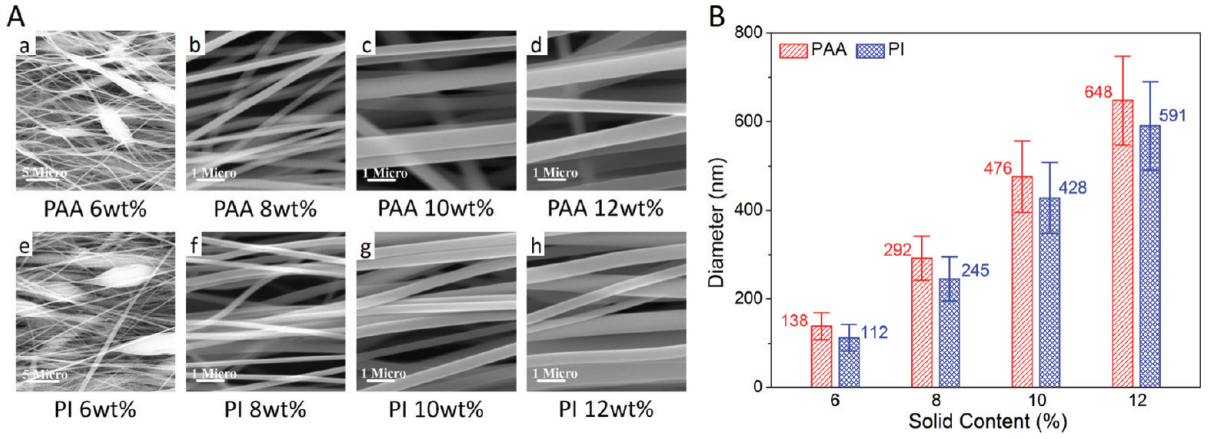

Figure 1. (A) SEM images for the ultrafine PAA fibers and the corresponding PI nanofibers prepared from (a, e) 6 wt % PMDA/ODA PAA solution, (b, f) 8 wt % PMDA/ODA PAA solution, (c, g) 10 wt % PMDA/ODA PAA solution, and (d, h) 12 wt % PMDA/ODA PAA solution, and (B) the diameter variations of the ultrafine fibers with the concentration of the PAA solutions. The as-spun ultrafine PAA fibers were cyclodehydrated to the corresponding ultrafine PI fibers by being thermally treated to 300 °C over 2 h and then kept at 300 °C for 2 h.

viscometer with an internal capillary diameter of 0.58 mm. The intrinsic viscosity of the synthesized PAA was determined by first measuring the viscosities of a series of dilute PAA solutions with concentrations of 0.5, 1.0, 1.5, and 2.0 mg mL^{-1} followed by extrapolating the concentration of the PAA solution to zero according to eq 1 ($\eta_{sp}/c = [\eta] + k'[\eta]^2c$, where η_{sp} is the specific viscosity and c is the concentration) and eq 2 ($\ln \eta_r/c = [\eta] - k''[\eta]^2c$, where η_r is the relative viscosity).

The amount of silver(I) loaded into the PAA membranes was quantified with a Seiko Instruments SPS 8000 inductively coupled plasma (ICP) atomic emission spectrometer. The measurements were performed after the silver-doped PAA membranes had been dissolved in a 5 wt % nitric acid solution.

Attenuated total reflection-Fourier transform infrared (ATR-FTIR) spectra of the films were collected using a Nicolet Nexus670 IR spectrometer. Surface morphologies were recorded on a Hitachi S-4700 field-emission scanning electron microscope (FE-SEM) operating at 20 kV. The samples were coated with ca. 5 nm of platinum prior to the measurements.

The silver nanoparticles on the surface of the ultrafine fibers were observed using a JEOL JEM-2200FS transmission electron microscope (TEM) at an accelerating voltage of 200 kV. Samples for TEM observations were prepared by depositing samples on carbon-coated copper grids.

X-ray diffraction (XRD) data were recorded on a Bruker AXS D8 ADVANCE X-ray diffractometer (Karlsruhe, Germany) in the 10–90° range at a scanning rate of 10° min^{-1}. The X-ray beam was generated by a Cu Kα target with a wavelength of 0.154056 nm, using a tube voltage of 40 kV and a current of 40 mA.

X-ray photoelectron spectra (XPS) were collected using an ESCALAB 250 spectrometer (Thermo Electron Corporation) in the fixed analyzer transmission mode. The instrument is equipped with a monochromatic Al Kα X-ray source and a magnetic lens system that yields high spatial resolution and high sensitivity. A takeoff angle of 45° was used to obtain most of the spectra. The pressure in the analysis chamber was maintained at 2×10^{-10} mbar or lower during each measurement. Surface elemental compositions were calculated from the peak area ratios on the XPS spectra. Thermogravimetric analysis (TGA) was performed by a TA Q50 system at a heating rate of 10 K·min^{-1}.

RESULTS AND DISCUSSION

Characterization of the As-Spun Ultrafine PAA Fibers. To obtain ultrafine poly(amic acid) precursor ultrafine fibers with desirable morphologies, PAA solutions with different concentrations were employed for electrospinning. Figure 1 shows the SEM images and the diameter variations of the as-spun ultrafine PAA fibers and the corresponding PI nanofibers derived from the 6, 8, 10, and 12 wt % PAA solutions. As can be observed, all the ultrafine fibers are aligned very well on the graphite paper substrate, and the average diameters for the PAA and PI ultrafine fibers were continually decreased with the reduced concentration. For the PAA solutions with 12 wt %, ultrafine PAA fibers were electrospun with an average diameter of 648 ± 100 nm, and the PI fibers obtained after cyclodehydration were 591 ± 100 nm, while for the 8 wt % solution, the ultrafine fibers were prepared with 292 ± 50 nm in diameter for the PAA and 245 ± 50 nm in diameter for the corresponding PI. This indicates that the concentration of the PAA solutions has significant effect on the ultrafine fibers' diameters. Further decrease in the PAA concentrations leads to the formation of thinner ultrafine PAA fibers. However, experimental results indicates that beads were inevitably formed in the nonwoven fabric membranes when the PAA solutions were diluted to below 8 wt %, as can be observed in the SEM image in Figure 1a (6 wt % PAA). Thus, the ultrafine fiber membranes prepared from the 8 wt % PAA solution were chosen as the precursor fibers for the followed ion exchange.

Ion Exchange. Because of the presence of many active carboxylic acid groups in the PAA macromolecules, PAAs have significantly higher cation-complexing abilities than their imide forms.[49,50] This characteristic allows for the in situ reactions of PAA with the salts of noble metals having labile anions to generate a metal–polymeric blend. In our previous works, by simply immersing the PAA in aqueous silver(I) solutions, it has been demonstrated that silver ions could be readily introduced into the PAA films (30–50 μm thick) through the coordination of the negatively charged polycarboxylate groups with the positive silver ions to form a silver polycarboxylate salt, silver polyamate, in the precursor films. Herein, by employing the same procedure, silver ions were successfully incorporated into our as-spun PAA ultrafine fibers. As quantified by ICP atomic emission spectroscopy, the silver(I) loaded into the PAA ultra fibers were 1.75, 2.26, and 2.54 wt %, respectively, for the nonwoven PAA fabrics treated in a 0.01 M $[Ag(NH_3)_2]^+$ aqueous solution for 10, 15, and 20 s. Correspondingly, the XPS composition data in Table 1 indicate that the amount of silver ions mounted on the PAA ultrafine fibers' surface reached levels of 1.30, 2.07, and 2.11 atom %, respectively. These results indicate that $[Ag(NH_3)_2]^+$ is a high efficient silver source for

dx.doi.org/10.1021/am300248c | ACS Appl. Mater. Interfaces 2012, 4, 2583–2590

Table 1. XPS Surface Composition Data for the PAA Nanofibers Ion Exchanged in 0.01 M Aqueous $[Ag(NH_3)_2]^+$ Solution for Varying Time

	relative atomic concentration (atom %)			
ion exchange time (s)	C 1s	O 1s	N 1s	Ag 3d
0	75.51	21.24	3.25	0.00
10	73.63	21.68	3.39	1.30
15	75.12	19.65	3.16	2.07
20	74.11	21.12	2.66	2.11

ion exchange, and the rapid and efficient loading of silver(I) into the ultrafine fibers are supposed to be attributed to the alkaline nature of the $[Ag(NH_3)_2]^+$ solution and the high specific surface area of the ultrafine fibers, both of which have positive effects on accelerating the reaction of carboxylic acid groups with metal ions, whereas due to the existence of hydrolyzable amide groups in the PAA ultrafine fibers, the loading of silver via ion exchange was inevitably accompanied by the hydrolysis and degradation of the polymer chains, especially in alkaline environments.[49] Considering the ultrafine diameters of the electrospun fibers, a $[Ag(NH_3)_2]^+$ solution of only 0.01 M (pH 9.9−10.2) was selected in the present work, and the ion exchange time was confined to no more than 20 s to prevent the occurrence of serious damages on the fibers. A 0.02 M $[Ag(NH_3)_2]^+$ solution was used to load silver(I) ions and also ion exchange for 25 s with the ultrafine PAA fibers at the concentration of 0.01 M $[Ag(NH_3)_2]^+$ solution to fabricate PI ultrafine fibers doped with silver nanoparticles. Figures S1 and S2 of the Supporting Information show the corresponding SEM images. The cross-linking phenomenon after the ultrafine fibers of PAA mats ion exchange with 0.02 M $[Ag(NH_3)_2]^+$ solution or ion exchange for 25 s was more serious.

Figure 2 shows the ATR-FTIR spectra for the pure ultrafine PAA fiber and its catalogues after ion exchange in the 0.01 M

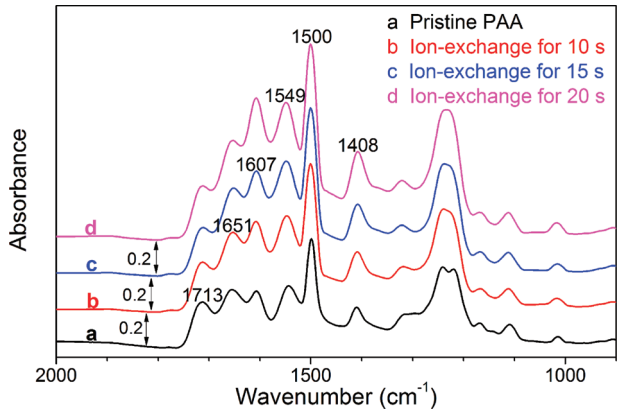

Figure 2. ATR-FTIR spectra for the pure PAA nanofibers and the silver(I)-doped PAA nanofibers prepared by immersing the pure ultrafine PAA fibers in a 0.01 M $[Ag(NH_3)_2]^+$ solution for 10, 15, and 20 s.

$[Ag(NH_3)_2]^+$ aqueous solution for different times. The absorbance observed at 1713 cm^{-1} is corresponding to the C═O vibrations of the carboxylic acid groups,[48,49,51] while the peaks locating at 1651 and 1549 cm^{-1} are related to the vibrational mode of the amide groups. The appearance of these peaks indicates the amic acid characteristics of the PAA ultrafine fibers. The C═O symmetrical and asymmetrical stretching vibrations in $-COO^-$ are located at 1607 and 1408 cm^{-1}, respectively.[51] To evaluate the structure variations occurring in the PAA ultrafine fibers during ion exchange, the absorbance intensities of all the above-mentioned characteristic peaks were quantitatively deliberated using the absorbance of the benzene ring at 1500 cm^{-1} as the internal standard, the results of which were shown in Table 2. As observed, the

Table 2. IR Intensity Variations as a Function of Ion Exchange Time for the Absorbances at 1408, 1607, 1651, and 1713 cm^{-1} Using the Benzene Ring Absorbance at 1500 cm^{-1} as the Internal Standard

ion exchange time (s)	I_{1408}/I_{1500}[a]	I_{1607}/I_{1500}	I_{1651}/I_{1500}	I_{1713}/I_{1500}
0	0.63	0.62	0.86	0.59
10	0.65	0.69	0.68	0.37
15	0.70	0.71	0.66	0.29
20	0.74	0.88	0.60	0.28

[a] I_{1408}/I_{1500} means the intensity ratio of the absorbance at 1408 and 1500 cm^{-1}.

absorbance at 1713 cm^{-1} (−COOH) was gradually decreased with increasing ion exchange time. This is suggested to correspond to the gradual dissociation of the carboxylic acid groups and the formation of the silver-carboxylate, as verified by the continually enhanced 1408 and 1607 cm^{-1} absorbances ($-COO^-$). Besides, the 1651 cm^{-1} amide peak was gradually degraded with increasing ion exchange times, which is ascribed to the hydrolysis of the amide groups. This is to be expected since our previous works[49] have demonstrated that ion exchange in silver ion aqueous solutions will cause inevitable hydrolysis of the PAA macromolecules, especially in the alkaline $[Ag(NH_3)_2]^+$ aqueous solution. However, under the present experimental conditions with ion exchange times no more than 20 s, all the ion exchanged PAA ultrafine fibers exhibit almost the same IR spectra with that of the pure ultrafine PAA fibers, suggesting the well maintenance of the essential poly(amic acid) structures, consistent with the almost unaltered C, N, and O XPS atomic concentrations observed in Table 1.

Thermal Imidization and Silver Reduction. SEM images for the pure ultrafine PAA fibers before and after ion exchange in $[Ag(NH_3)_2]^+$ solution were shown in Figure 3a−c. The as-spun ultrafine PAA fibers exhibit fairly well alignment on the substrate, as observed in Figure 3 a. However, Figure 3b,c indicates that the well-aligned ultrafine PAA fibers basically lost their orientations after ion exchange. This is out of our expectation and is suggested to be due to the shrinkage of the ultrafine PAA fibers occurring during the loading of silver(I) via ion exchange. Fortunately, the morphologies of the ultrafine PAA fibers such as the diameters and the surfaces are well-retained and do not show any discernible damages after ion exchange.

For preparing ultrafine PI fibers embedded with silver nanoparticles, thermal treatment was then carried out on the silver(I)-doped PAA precursor ultrafine fibers. Thermal curing converts the PAA into its final PI form with the concomitant silver reduction and aggregation, producing the silver-PI hybrid nanofibers. The ideal chemistry involved in the heat treatment process was depicted in Scheme 1. Both inert and air atmospheres were investigated during thermal treatment. However, it should be noted that silver-nanoparticle-incorporated ultrafine PI fibers were only obtained under an inert

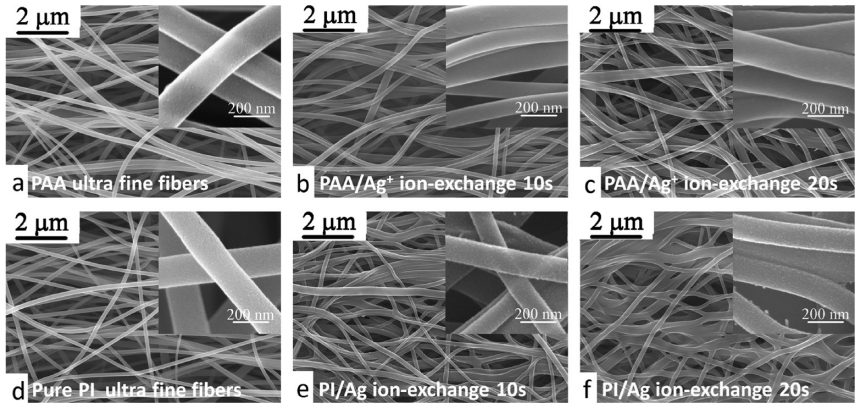

Figure 3. FE-SEM images for the ultrafine PAA fibers ion exchange in 0.01 M aqueous $[Ag(NH_3)_2]^+$ solution for different times and the corresponding PI nanofibers with silver nanoparticles, (a, d) ion exchanged in 0.01 M aqueous $[Ag(NH_3)_2]^+$ solution for 0 s, (b, e) ion exchanged in 0.01 M aqueous $[Ag(NH_3)_2]^+$ solution for 10 s, and (c, f) ion exchanged in 0.01 M aqueous $[Ag(NH_3)_2]^+$ solution for 20 s.

environment in the present work. Under air conditions, the precursor ultrafine fibers underwent a serious decomposition process probably due to the serious catalytic and oxidative degradation effect of the reduced silver nanoparticles.[41,43,49] Figure 3d–f shows the SEM images of the ultrafine PI fibers and PI–Ag fibers obtained after thermal treatment under N_2 environments. For the pure PI nonwoven fabric membranes (Figure 3d), ultrafine fibers with good uniformity were obtained and the morphologies of the fibers do not show obvious changes after thermal treatment except the diameter thinning as compared to the precursor ultrafine fibers (Figure 3a). However, significant morphology variations were observed on the silver(I)-doped fiber membranes after thermal treatment. For the one ion exchanged in the 0.01 M $[Ag(NH_3)_2]^+$ solution for 10 s, the obtained ultrafine PI fibers were considerably fused together in the nonwoven fabric membranes forming an apparently more compact fiber network, as observed in Figure 3e. Plenty of connection points (or cross-linking points) were observed in the membrane, which were significantly increased after extending the ion exchange time to 20 s. In addition, the results show that the alignment of the silver-doped fibers was completely lost after thermal treatment, suggesting the serious and continually occurring shrinkage of the fibers during cycloimidization.

Nevertheless, the enlarged SEM images in Figure 3e,f indicate that silver nanoparticles with sizes around 20 nm are uniformly embedded on the surface of the ultrafine fibers, indicating the successful fabrication of the silver-nanoparticle-incorporated PI nanofibers. Figure 4 shows the TEM images for the PI–Ag nanofibers prepared by thermally treating the precursor PAA ultrafine fibers ion exchanged in silver ion solution for 20 s. As shown, silver nanoparticles with sizes in the range of 5–20 nm were evenly distributed on the surface of the finally imidized PI ultrafine fibers. Serious silver agglomeration was not observed, and it is suggested that it is the chemically (i.e., ion exchange) loaded silver ions in the precursor ultrafine fibers that facilitate the silver reduction and nucleation but limit the subsequent particle agglomerating due to the strong polymer–metal interactions, resulting in the formation of the small-sized particles and their uniform distribution. To this point, it is concluded that the ultrafine PI fibers embedded with silver nanoparticles were successful fabricated in our current work via the direct ion exchange self-metallization process, and the enlarged SEM images in Figure 3e,f and the TEM images in Figure 4 suggest that most of the

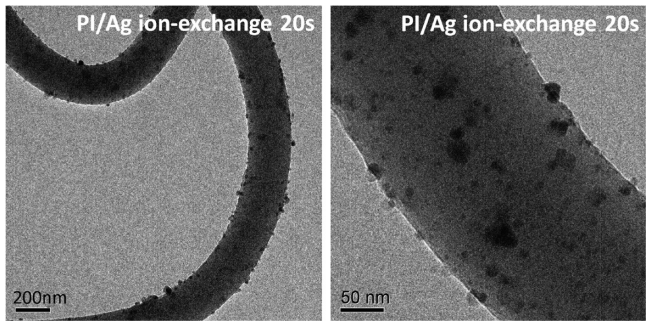

Figure 4. TEM images of the silver-doped ultrafine PI fibers prepared from the PAA nanofibers ion exchanged in a 0.01 M silver ammonia solution for 20 s followed by being thermally cured in N_2 environment to 300 °C in 2 h and then held constant at 300 °C for 2 h.

silver nanoparticles are deposited on the surface of the ultrafine fibers.

The chemical states of the silver nanoparticles embedded in the ultrafine PI fibers are one of the primary concerns. Figure 5 shows the XRD spectrum for the PI–Ag hybrid nanofibers derived from the precursor ultrafine PAA fibers ion exchanged in 0.01 M silver ammonia solution for 10 s. The result reveals that silver nanoparticles were present in the form of face-centered cubic (fcc) crystals in the PI nanofiber mat. The

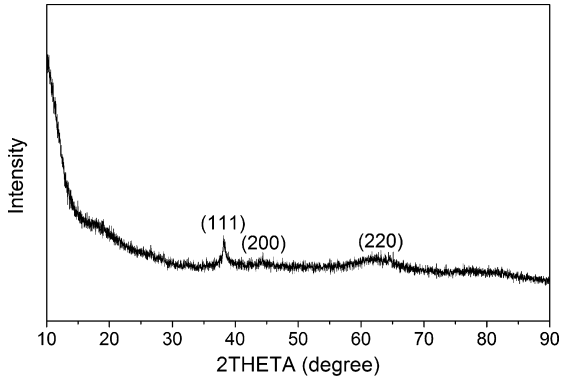

Figure 5. XRD pattern for the PI–Ag nanofibers prepared from the PAA fibers ion exchanged in a 0.01 M silver ammonia solution for 10 s followed by being thermally cured in N_2 environment to 300 °C in 2 h and then held constant at 300 °C for 2 h.

reflections with 2θ values at 38.2°, 44.3°, and 64.5° are corresponding to the (111), (200), and (220) crystal faces of the fcc silver, respectively. The average silver crystal size, as estimated from Scherrer equation using the full width at half-maximum (fwhm) of the strongest characteristic peak (111), is approximately 14.1 nm, a little smaller than those observed in the SEM and TEM images shown above (ca. 20 nm), suggesting the quite limited agglomeration of the formed silver crystals.

Thermal Characterization. In the present experiment, it should be mentioned that silver-nanoparticle-incorporated ultrafine PI fibers could be obtained only under inert environment. Under air conditions, the precursor ultrafine fibers underwent a serious decomposition process, which is suggested to be due to the serious catalytic and oxidative degradation effect of the reduced silver nanoparticles, as reported in literature.[41,43,49] For a better understanding of the chemistry involved in the thermal treatment process, constant-temperature thermal analyses were carried out on the silver(I)-doped PAA nanofibers in both nitrogen and air atmospheres.

Figure 6 shows the isothermal TGA results for the 20 s-silver-ion-exchanged PAA ultrafine fibers measured at a

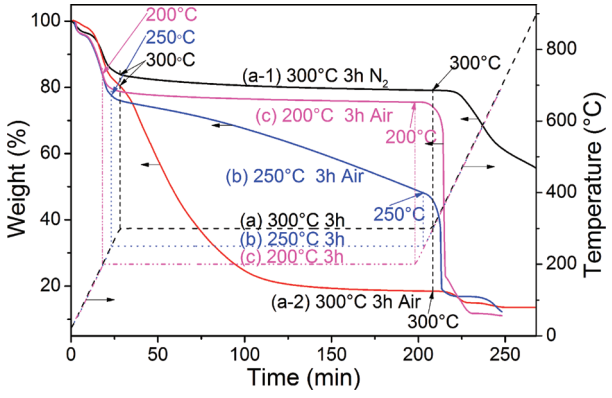

Figure 6. The isothermal TGA curves measured at different temperatures in nitrogen and air atmospheres for the PAA ultra fine fibers ion exchanged in a 0.01 M aqueous $[Ag(NH_3)_2]^+$ solution for 20 s.

constant temperature of 300 °C in N_2 and air, 250 °C in air, and 200 °C in air. For the silver(I)-PAA nanofibers measured at 300 °C under N_2 environment, the TGA curve (Figure 6a-1) exhibits a significant weight loss of about 15 wt % when rising the temperature from 25 to 300 °C, which is suggested to be due to the removal of the DMF solvent remaining in the ultrafine PAA fibers and the cyclodehydration of the PAA to its PI form. When keeping at 300 °C under N_2, the nanofibers exhibit considerably excellent thermal stability and do not show any distinguishable weight loss in the whole isothermal process (about 3 h). This indicates that thermal cycloimidization of the PAA ultrafine fibers were basically finished before 300 °C, and under N_2 atmosphere at 300 °C, the silver catalytic decomposition effect was used to tune the morphology and distribution of silver nanoparticles at the interfaces of ultrafine fibers.[52] However, the situation was completely different under air conditions. As shown in Figure 6a-2, a significant weight loss (ca. 19 wt %) was also observed before rising the temperature to 300 °C. However, the weight loss is about 4 wt % higher than that of the ultrafine fibers heated under N_2 (Figure 6a-1). Thus, it is anticipated that thermal degradation starts to occur in the nanofibers before 300 °C when being heated in air. Violent thermal decomposition was observed during the continued isothermal annealing process, and about 60 wt % of the ultrafine fibers were burned out in less than 100 min at 300 °C, leaving residues at around 20 wt %. These results indicate that silver has considerably significant catalytic effect on the decomposition of the polyimide nanofibers and oxygen plays an essential role in the degradation process. However, this violent silver-catalyzed degradation behavior could be effectively restricted by reducing the thermal treatment temperatures. As shown in Figure 6b, by limiting the isothermal temperature to 250 °C, the weight-loss speed during the isothermal process was considerably reduced. Further decreasing the temperature to 200 °C (Figure 6c), the ultrafine fibers do not show any weight loss during the whole isothermal process in air, indicating the extinction of the thermal decomposition. However, Figure 6b,c exhibits higher weight losses than that of the ultrafine fibers heated in N_2 (Figure 6a-1), suggesting that thermal degradation of the silver-doped fibers readily occurs in air even at relatively low temperatures.

To evaluate the influence of the incorporated silver nanoparticles on the thermal stabilities of the finally obtained hybrid nanofibers, TGA analyses were carried out. Figure 7

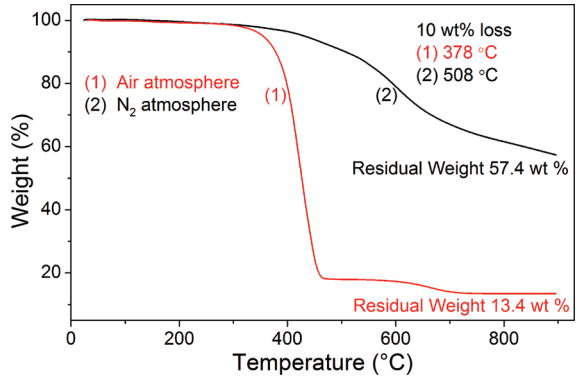

Figure 7. TGA curves in both air and nitrogen atmospheres for the silver-doped PI fibers obtained from the PAA ultrafine fibers ion exchanged in a 0.01 M aqueous $[Ag(NH_3)_2]^+$ solution for 20 s and cured in N_2 environment to 300 °C in 2 h and then held constant at 300 °C for 2 h.

shows the TGA curves for the silver-nanoparticle-incorporated PI nanofibers prepared by thermally treating the 20 s-ion exchanged ultrafine PAA fibers to 300 °C under N_2 environment. As can be observed, under N_2 environment, the PI–Ag ultrafine fibers exhibit very excellent thermal stability with a 10%-weight-loss temperature at 508 °C even though silver nanoparticles were included. However, in air, the degradation temperatures were considerably lowered (130 °C decrease), verifying the strong catalytic oxidative effect of the doped silver nanoparticles. Nevertheless, the silver-doped PI ultrafine fibers are still in the class of high-temperature materials and could meet the requirement for many practical high-temperature applications.

CONCLUSIONS

In this paper, ultrafine polyimide (PI) fibers incorporated with silver nanoparticles were successfully fabricated using silver ammonia complexcation ($[Ag(NH_3)_2]^+$) as the silver precursor and pyromellitic dianhydride (PMDA)/4,4′-oxidianiline (4,4′-ODA) polyimide as the matrix via the direct ion exchange self-

metallization technique. Our present work demonstrates that polyimide ultrafine fibers doped with silver nanoparticles were successfully fabricated via the direct ion exchange self-metallization technique. By employing a dilute silver ion solution with a concentration of 0.01 M as the silver sources and ion exchange time of less than 20 s, silver nanoparticles with sizes less than 20 nm were uniformly distributed on the surface of the ultrafine PI fibers. Thermal treatment environment plays a key role in the ultrafine fiber preparation process. Serious decomposition occurred when treating silver(I)-doped precursor fibers under air conditions, and the silver-nanoparticle-incorporated ultrafine PI nanofibers were only obtained under inert atmospheres in the present experiment. Although the thermal decomposition of the hybrid fibers at 10% weight loss in air were decrease about 130 °C after silver incorporation, the finally obtained PI−Ag ultrafine fibers still possess a high thermal stability (378 °C), which is adequate for many high-temperature applications. The present work provides an efficient and simple approach for the preparation of silver-nanoparticle-incorporated ultrafine PI fibers.

■ ASSOCIATED CONTENT

Ⓢ Supporting Information

The SEM images of PI nanofibers doped with silver nanoparticles.This material is available free of charge via the Internet at http://pubs.acs.org.

■ AUTHOR INFORMATION

Corresponding Author

*Tel.:+86 10 6442 4654. Fax: +86 10 6442 1693. E-mail: qisl@mail.buct.edu.cn.

Notes

The authors declare no competing financial interest.

■ ACKNOWLEDGMENTS

The authors acknowledge financial support from the National Natural Science Foundation of China (NSFC, Contract Grant No. 50903006, 51071015) and the Specialized Research Fund for the Doctoral Program of Higher Education (SRFDP, Project No. 20090010120008).

■ REFERENCES

(1) Huang, Z. M.; Zhang, Y. Z.; Kotaki, M.; Ramakrishna, S. *Compos. Sci. Technol.* **2003**, *63*, 2223.
(2) Kim, G.; Kim, W. *Appl. Phys. Lett.* **2006**, 88.
(3) Thavasi, V.; Singh, G.; Ramakrishna, S. *Energy Environ. Sci.* **2008**, *1*, 205.
(4) Schreuder-Gibson, H.; Gibson, P.; Senecal, K.; Sennett, M.; Walker, J.; Yeomans, W.; Ziegler, D.; Tsai, P. P. *J. Adv. Mater.* **2002**, *34*, 44.
(5) Frey, M. W.; Li, L. *J. Eng. Fibers Fabr.* **2007**, *2*, 31.
(6) Parajuli, D. C.; Bajgai, M. P.; Ko, J. A.; Kang, H. K.; Khil, M. S.; Kim, H. Y. *ACS Appl. Mater. Interfaces* **2009**, *1*, 750.
(7) Park, S. W.; Bae, H. S.; Xing, Z. C.; Kwon, O. H.; Huh, M. W.; Kang, I. K. *J. Appl. Polym. Sci.* **2009**, *112*, 2320.
(8) Zhang, S.; Shim, W. S.; Kim, J. *Mater. Design.* **2009**, *30*, 3659.
(9) Demir, M. M.; Yilgor, I.; Yilgor, E.; Erman, B. *Polymer* **2002**, *43*, 3303.
(10) Tsai, P. P.; Schreuder-Gibson, H.; Gibson, P. *J. Electrost.* **2002**, *54*, 333.
(11) Zhuo, H.; Hu, J.; Chen, S.; Yeung, L. *J. Appl. Polym. Sci.* **2008**, *109*, 406.
(12) Bognitzki, M.; Hou, H. Q.; Ishaque, M.; Frese, T.; Hellwig, M.; Schwarte, C.; Schaper, A.; Wendorff, J. H.; Greiner, A. *Adv. Mater.* **2000**, *12*, 637.
(13) Krishnappa, R. V. N.; Sung, C. M.; Schreuder-Gibson, H. In *Advanced Fibers, Plastics, Laminates and Composites*; Materials Research Society: Warrendale, PA, 2002; Vol. *702*, p 235.
(14) Shawon, J.; Sung, C. M. *J. Mater. Sci.* **2004**, *39*, 4605.
(15) Yang, D.; Wang, Y.; Zhang, D.; Liu, Y.; Jiang, X. *Chin. Sci. Bull.* **2009**, *54*, 2911.
(16) Dzenis, Y.; Wen, Y. K. In *Advanced Fibers, Plastics, Laminates and Composites*; Materials Research Society: Warrendale, PA, 2002; Vol. *702*, p 173.
(17) Feng, L.; Li, S. H.; Li, H. J.; Zhai, J.; Song, Y. L.; Jiang, L.; Zhu, D. B. *Angew. Chem., Int. Ed.* **2002**, *41*, 1221.
(18) Wang, Y.; Serrano, S.; Santiago-Aviles, J. J. *J. Mater. Sci. Lett.* **2002**, *21*, 1055.
(19) Wang, T.; Kumar, S. *J. Appl. Polym. Sci.* **2006**, *102*, 1023.
(20) Ding, B.; Kim, H. Y.; Lee, S. C.; Shao, C. L.; Lee, D. R.; Park, S. J.; Kwag, G. B.; Choi, K. J. *J. Polym. Sci. Polym. Phys.* **2002**, *40*, 1261.
(21) Koski, A.; Yim, K.; Shivkumar, S. *Mater. Lett.* **2004**, *58*, 493.
(22) Tao, J.; Shivkumar, S. *Mater. Lett.* **2007**, *61*, 2325.
(23) Bognitzki, M.; Czado, W.; Frese, T.; Schaper, A.; Hellwig, M.; Steinhart, M.; Greiner, A.; Wendorff, J. H. *Adv. Mater.* **2001**, *13*, 70.
(24) Caruso, R. A.; Schattka, J. H.; Greiner, A. *Adv. Mater.* **2001**, *13*, 1577.
(25) Zhou, H.; Green, T. B.; Joo, Y. L. *Polymer* **2006**, *47*, 7497.
(26) Touny, A. H.; Lawrence, J. G.; Jones, A. D.; Bhaduri, S. B. *J. Mater. Res.* **2010**, *25*, 857.
(27) Kim, C.; Choi, Y. O.; Lee, W. J.; Yang, K. S. *Electrochim. Acta* **2004**, *50*, 883.
(28) Zhang, Q.; Wu, D. Z.; Qi, S. L.; Wu, Z. P.; Yang, X. P.; Jin, R. G. *Mater. Lett.* **2007**, *61*, 4027.
(29) Hu, N. T.; Dang, G. D.; Zhang, H. N.; Du, Y.; Wang, C.; Zhou, H. W.; Meng, X. H.; Chen, C. H. *J. Nanosci. Nanotechnol.* **2009**, *9*, 6688.
(30) Xuyen, N. T.; Jeong, H. K.; Kim, G.; So, K. P.; An, K. H.; Lee, Y. H. *J. Mater. Chem.* **2009**, *19*, 1283.
(31) Carlberg, B.; Ye, L.-L.; Liu, J. *Small* **2011**, *7*, 3057.
(32) Givens, S. R.; Gardner, K. H.; Rabolt, J. F.; Chase, D. B. *Macromolecules* **2007**, *40*, 608.
(33) Rein, D. M.; Shavit-Hadar, L.; Khalfin, R. L.; Cohen, Y.; Shuster, K.; Zussman, E. *J. Polym. Sci. Polym. Phys.* **2007**, *45*, 766.
(34) Lee, K. H.; Ohsawa, O.; Watanabe, K.; Kim, I. S.; Givens, S. R.; Chase, B.; Rabolt, J. F. *Macromolecules* **2009**, *42*, 5215.
(35) Hao, M.; Liu, Y.; He, X.; Ding, Y.; Yang, W. In *Advanced Polymer Science and Engineering*; Trans Tech Publications Inc.: Durnten-Zurich, Switzerland, 2011; Vol. *221*, p 129.
(36) Jin, W. J.; Lee, H. K.; Jeong, E. H.; Park, W. H.; Youk, J. H. *Macromol. Rapid Commun.* **2005**, *26*, 1903.
(37) Ganeev, R.; Baba, M.; Ryasnyansky, A.; Suzuki, M.; Kuroda, H. *Opt. Commun.* **2004**, *240*, 437.
(38) Moura, M. R.; Mattoso, L. H. C.; Zucolotto, V. *J. Food Eng.* **2012**, *109*, 520.
(39) Lin, J. J.; Lin, W. C.; Dong, R. X.; Hsu, S. H. *Nanotechnology* **2012**, *23*, 065102.
(40) Shukla, M. K.; Singh, R. P.; Reddy, C. R. K.; Jha, B. *Bioresour. Technol.* **2012**, *107*, 295.
(41) Southward, R. E.; Thompson, D. S.; Thompson, D. W.; Clair, A. K. S. *Chem. Mater.* **1999**, *11*, 501.
(42) Sun, L.; Zhang, Z.; Dang, H. *Mater. Lett.* **2003**, *57*, 3874.
(43) Zhang, F.; Guan, N.; Li, Y.; Zhang, X.; Chen, J.; Zeng, H. *Langmuir* **2003**, *19*, 8230.
(44) Gan, X.; Liu, T.; Zhong, J.; Liu, X.; Li, G. *ChemBioChem* **2004**, *5*, 1686.
(45) Son, W. K.; Youk, J. H.; Lee, T. S.; Park, W. H. *Macromol. Rapid Commun.* **2004**, *25*, 1632.
(46) Doty, R. C.; Tshikhudo, T. R.; Brust, M.; Fernig, D. G. *Chem. Mater.* **2005**, *17*, 4630.

(47) Qi, S.; Wu, Z.; Wu, D.; Wang, W.; Jin, R. *Chem. Mater.* **2007**, *19*, 393.
(48) Qi, S.; Wu, Z.; Wu, D.; Wang, W.; Jin, R. *Langmuir* **2007**, *23*, 4878.
(49) Qi, S.; Wu, Z.; Wu, D.; Jin, R. *J. Phys. Chem. B* **2008**, *112*, 5575.
(50) Qi, S.; Wu, Z.; Wu, D.; Yang, W.; Jin, R. *Polymer* **2009**, *50*, 845.
(51) Jin, Y.; Zeng, G. F.; Zhu, D. Y.; Huang, Y.; Su, Z. H. *Chin. J. Appl. Chem.* **2011**, *28*, 258.
(52) Akamatsu, K.; Shinkai, H.; Ikeda, S.; Adachi, S.; Nawafune, H.; Tomita, S. *J. Am. Chem. Soc.* **2005**, *127*, 7980.